Journal of Magnetic Resonance **140,** 84–90 (1999)
Article ID jmre.1999.1824, available online at http://www.idealibrary.com on IDEAL®

Feedback Optimization of Pulse Width in the SORC Sequence

J. L. Schiano,* T. Routhier,† A. J. Blauch,* and M. D. Ginsberg‡

**Department of Electrical Engineering, The Pennsylvania State University, 227D Electrical Engineering West, University Park, Pennsylvania 16802; †United States Coast Guard Command and Control Engineering Center, Portsmouth, Virginia 23703; and ‡United States Army Construction Engineering Research Laboratories, P.O. Box 9005, Champaign, Illinois 61826*

Received October 2, 1998; revised May 10, 1999

A method for increasing the signal-to-noise ratio (SNR) of nuclear quadrupole resonance (NQR) measurements by automatically adjusting a pulse parameter in real-time is presented. This approach is useful in situations where the optimal pulse parameters cannot be chosen beforehand due to lack of knowledge regarding the system. For example, NQR provides a means for detecting explosives by revealing the presence of ^{14}N. In this particular application, the distance between the search coil and the explosive, as well as the temperature of the explosive, is unknown. As a result, a fixed set of pulse parameters will not yield the largest SNR for all possible search applications. This paper describes a feedback algorithm that uses measurements of the NQR signal to automatically adjust the pulse width in the strong off-resonant comb sequence to maximize the SNR of the NQR measurement. Experimental results obtained using a sample of sodium nitrite are presented.

Key Words: **nuclear quadrupole resonance; strong off-resonant comb sequence; pulse parameter optimization; feedback control; gradient method.**

1. INTRODUCTION

Nuclear quadrupole resonance (NQR) has been investigated as a means for detecting both explosives and narcotics by revealing the presence of ^{14}N (*1, 2*). Although ^{14}N is essentially 100% abundant, the small zero-field NQR splitting results in a low signal-to-noise ratio (SNR). As a result, in order to increase the probability of detection it is necessary to improve the SNR of NQR measurements.

One method for increasing the SNR is to coherently add consecutive NQR signals produced by a multipulse sequence (*3–5*). Examples include the phase-alternated (PAPS) (*6*), non-phase-alternated (NPAPS) (*6*), spin-locked spin echo (SLSE) (*4*), and strong off-resonant comb (SORC) (*7*) pulse sequences. The amplitude of the NQR signal in multipulse sequences is sensitive to pulse sequence parameters such as pulse width, pulse separation, and frequency. Because the optimum pulse parameters are determined by unknown factors such as the location of the mine with respect to the search coil and the temperature of the explosive, one cannot obtain the maximum SNR for all regions by using a fixed set of pulse parameters (*8*). Suboptimal pulse parameters can result in a significant loss in SNR, thereby decreasing the probability of a successful detection.

Although the optimal value of a given pulse parameter is unknown a priori, the range in which it lies can be estimated. Smith (*9*) used this fact to develop a sequence that partially overcomes the dependence of the NQR signal amplitude on environmental factors such as temperature. The sequence uses several different sets of pulse parameters which cover the range containing the optimal value. The set closest to the optimal value yields the largest NQR signal. For example, several RF pulses are applied in succession, each with a different frequency and/or pulse width. The spacing between pulses is chosen so that the FID from the first pulse decays before the second pulse is applied. After allowing the system to relax back toward thermal equilibrium, the sequence of pulses is then repeated. The NQR signals following pulses of the same frequency and duration are averaged. The pulses with the frequency and duration nearest the optimal values yield the largest NQR signal. By increasing the number of different frequencies and/or widths used, it is possible to obtain a set that closely matches the optimal values. On the other hand, the need to acquire multiple NQR signals for averaging places a practical limitation on the number of different frequencies and pulses widths that can be incorporated into the pulse sequence. As a result, this approach has limited ability to account for variations in environmental parameters.

This paper presents a method for automatically calibrating a single pulse parameter. Using measurements of the NQR response between RF pulses, a feedback algorithm adjusts a pulse parameter so that the SNR of subsequent NQR measurements is increased. This method will enable a nontechnical operator to quickly calibrate a NQR detection system. Before beginning a search, the operator would place the NQR detection system over a buried test mine so that the feedback algorithm can determine the optimal pulse parameters for the particular explosive material, depth, size, and environmental conditions (i.e., temperature and soil composition).

The use of feedback to automatically optimize pulse parameters extends beyond the application to NQR. In fact,

1090-7807/99 $30.00

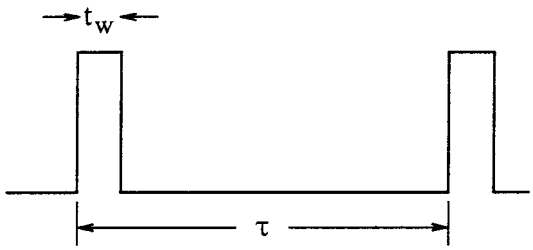

FIG. 1. The SORC sequence is a train of RF pulses with width t_w and spacing τ.

applications of feedback to MRI have already been investigated (*10–12*). The similarity of NMR and NQR techniques suggests that feedback concepts may also be applicable to NQR. As a first step we developed a simple method for automatically optimizing the pulse width in the strong off-resonant pulse sequence.

The SORC sequence is a series of off-resonant RF pulses separated by equal spacings that yields a steady-state signal periodic in the pulse repetition period (*7, 13*). Periodic excitation is desirable since it results in a periodic response that can be averaged to improve the signal-to-noise ratio. However, the amplitude of the NQR signal is reduced by repetitive application of RF pulses. The advantage of the SORC sequence is that the signals obtained are comparable in magnitude to the FID obtained from a fully relaxed system.

Figure 1 shows a SORC sequence with pulse width t_w and pulse spacing τ. For small values of pulse spacing, the NQR signal (Type I signal) following the kth pulse can interfere constructively with the spin echo (Type II signal) arising prior to the application of the $(k + 1)$th pulse. The condition for constructive interference is $\Delta f\tau = n + \frac{1}{2}$, where Δf is the offset from resonance and n is an integer (*7*). If $\Delta f\tau$ is an integer, destructive interference reduces the signal amplitude. Additionally, the SORC signal amplitude is sensitive to the pulse width. This paper demonstrates that measurements of the NQR signal can be used to automatically adjust the pulse width so that the SORC signal amplitude is maximized.

2. METHOD AND MATERIALS

The experiments were performed using a 70-g sample of sodium nitrite ($NaNO_2$), finely ground to avoid the generation of piezoelectric signals (*14*). The sample of sodium nitrite was packed into a 1-inch-diameter, 4-inch-long glass vial over which the probe coil was tightly wound. Experiments were performed at room temperature, and the frequency of the RF pulses is chosen 3.5 kHz above the $\nu_- = 3.600$ MHz NQR transition of ^{14}N. Except as noted, the pulse separation in the SORC sequence is fixed at 1 ms. The ν_- transition is dominated by a single spin–lattice relaxation time T_{1l} of 304 ms which is measured using the method of progressive saturation. A spin–spin relaxation time T_2 of 5.9 ms is measured using a two-pulse spin-echo decay. The spin-echo signal yields an estimate of 1.1 ms for the lineshape parameter T_2^*. A 1-kW pulsed spectrometer specifically designed for implementing feedback algorithms is used to obtain the NQR measurements. An important feature of this spectrometer is the ability to change pulse sequence parameters while the experiment is in progress.

3. CONTROL DESIGN

The process of generating an NQR signal using the SORC sequence can be viewed as a dynamic system whose input is the pulse width and whose output is the peak-to-peak voltage of the SORC signal. The control objective is to find the pulse width that maximizes the steady-state NQR measurement using present and past measurements of the SORC signal. The pulse width of the kth RF pulse is denoted as $t_w(k)$. Similarly, the peak-to-peak voltage of the SORC signal measured between the kth and $k + 1$th RF pulse is denoted as $V(k)$. The separation τ between consecutive RF pulses and the frequency of excitation are assumed to be fixed.

In most situations, signal averaging is required to detect an NQR signal. A SORC sequence that incorporates both averaging and feedback optimization of pulse width is shown in Fig. 2. Between the discrete-time indices k and $k + 1$ there are $N +$

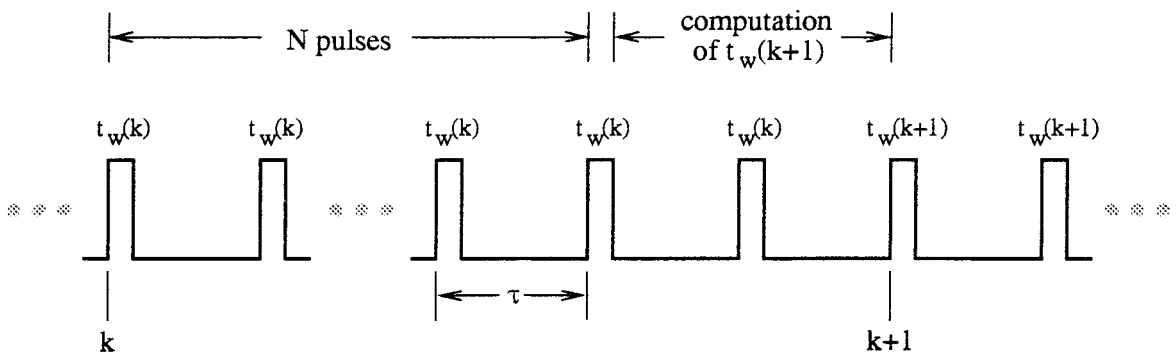

FIG. 2. SORC pulse sequence used in the control experiments.

2 RF pulses of fixed width $t_w(k)$ and pulse spacing τ. The first N SORC signals following the kth pulse are coadded to produce a single, averaged, SORC response whose peak-to-peak amplitude is denoted as $V_{avg}(k)$. During the interval 2τ following the acquisition of the Nth SORC signal, the feedback algorithm uses the measured signals $V_{avg}(k)$ and $V_{avg}(k-1)$ to determine the next pulse width $t_w(k+1)$.

Design of the feedback control algorithm must take into consideration that the signal $V_{avg}(k)$ is obtained by coadding N consecutive SORC responses that are obtained with fixed pulse width $t_w(k)$. If the period $\tau(N+2)$ between updates in the pulse width is three to five times longer than the dominant time constant of the SORC response to a change in pulse width, then the dynamics of the SORC signal are not critical in the design of the control algorithm. In effect, the design reduces to a problem in static optimization. This situation is advantageous in that uncertainty in T_1, T_2, and T_2^* will not affect the performance of the control algorithm. On the other hand, if the time $\tau(N+2)$ is small compared to the dominant time constant, then the dynamics of the NQR process must be considered in the design of the feedback algorithm. Despite efforts to model multipulse NQR sequences (*5, 15–17*), we are unaware of either a theoretical or an experimental study that describes the transient response of the SORC signal to a change in pulse width. Before considering the control design, the issue of SORC dynamics is first addressed.

3.1 SORC Response

The steady-state relationship between the amplitude of the SORC response and the pulse width t_w is measured for two different pulse separations. The system was allowed to reach steady-state over an interval of 3000 consecutive RF pulses. The subsequent 100 SORC signals are coadded to form an average SORC response. The peak-to-peak voltage V of the average SORC signal is used to describe the amplitude of the steady-state SORC signal.

Figure 3 shows the normalized amplitude of the steady-state SORC signal as a function of pulse width t_w for pulse spacings τ of 1 and 3 ms, which are chosen to produce constructive interference between the Type I and II signals. The amplitude is normalized with respect to the peak-to-peak voltage of a fully relaxed FID. In order to increase the amplitude of the NQR signal and the number of NQR signals available for averaging, the data show that a small pulse spacing is desirable. On the other hand, decreasing the pulse spacing also increases the sensitivity of the signal amplitude to the pulse width. This fact demonstrates the need for pulse width optimization.

Qualitative insight to the dynamic behavior of the SORC sequence is obtained by recording the transient response of the SORC signal to a step change in the pulse width. As an example, Fig. 4 shows the transient response of the SORC signal when the pulse width is increased from 6 to 12 μs. The vertical scale is normalized so that the SORC amplitude is

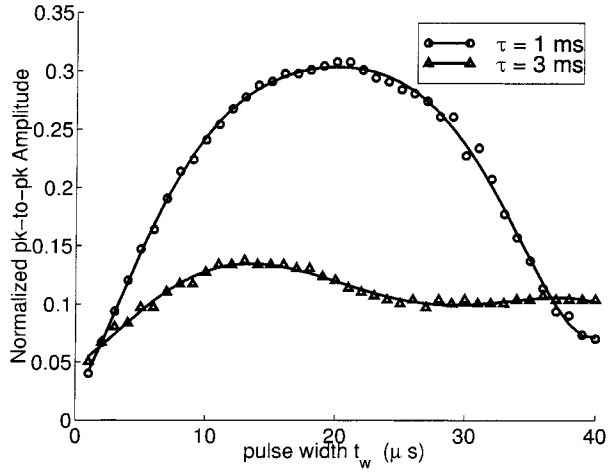

FIG. 3. Comparison of the steady-state SORC response as a function of pulse width, t_w for $\tau = 1$ and 3 ms.

unity for a pulse width of 12 μs. In order to improve the SNR, data from four identical experiments are averaged. The solid curve shows the steady-state SORC signal produced by the 6-μs pulse width. The dotted line shows the SORC signal immediately following the increase in pulse width, while the dashed–dotted curve shows the SORC signal 500 ms after the change in pulse width. The flat line at the beginning of each curve represents the delay time introduced by a lowpass filter in the receiver. The transient response in the SORC waveform occurs over an interval of T_2, and the system achieves a steady-state response within T_{1l} seconds. Also note that the locations of minima and maxima of the SORC signal remained fixed in the window between pulses despite the change in pulse width.

3.2 Gradient Method

Motivated by the sensitivity of the SORC amplitude to pulse width, we designed a feedback control system that adjusts the pulse width $t_w(k)$ to maximize the performance index

$$J(k) = \tfrac{1}{2}V_{avg}^2(k), \qquad [1]$$

where $V_{avg}(k)$ represents the peak-to-peak value of the average of N SORC signals obtained with a fixed pulse width $t_w(k)$. The pulse width that maximizes the performance index is found using the method of steepest ascent which is an iterative approach (*18*). The pulse width is updated using the rule

$$t_w(k+1) = t_w(k) + \lambda(k)\nabla_{t_w}J(k), \qquad [2]$$

where λ is a positive learning factor used to set the convergence rate, and $\nabla_{t_w}J(k)$ is the gradient of the performance index with respect to the pulse width t_w (*18*). This particular

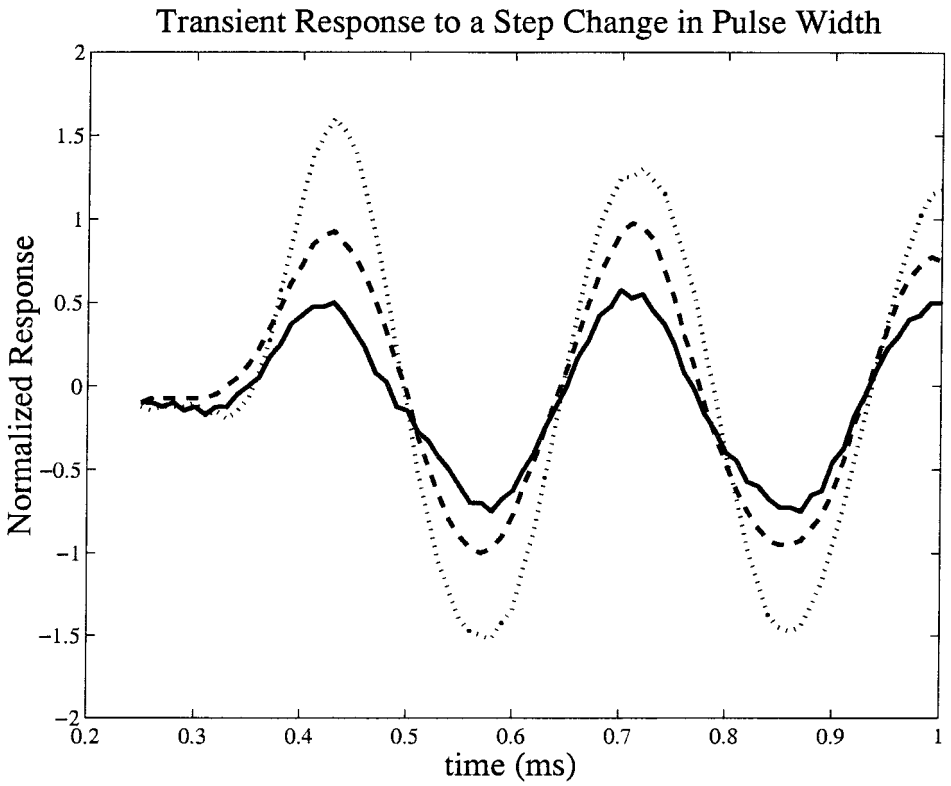

FIG. 4. Transient response of the SORC signal when the pulse width is stepped from 6 to 12 μs. The steady-state response of the SORC sequence for a fixed pulse width of 6 μs is indicated by the solid curve. The dotted curve shows the SORC signal immediately following the increase in pulse width from 6 μs to 12 μs. The dashed curve represents the SORC signal 500 ms after the step change in the pulse width.

approach for automatically adjusting the pulse width is called the gradient method (*19*).

The gradient $\nabla_{t_w} J(k)$ represents the ratio of the change in the peak-to-peak voltage of the average SORC signal to the change in pulse width. The low SNR of NQR measurements, even when averaging is used, results in poor performance when the gradient is approximated as

$$\nabla_{t_w} J(k) = \frac{V_{\text{avg}}(k) - V_{\text{avg}}(k-1)}{t_w(k) - t_w(k-1)}. \quad [3]$$

Instead, the gradient $\nabla_{t_w} J(k)$ is replaced by

$$\nabla_{t_w} J(k) = G(V_{\text{avg}}(k) - V_{\text{avg}}(k-1), \eta) \times G(t_w(k) - t_w(k-1), 0), \quad [4]$$

where $G(x, \eta)$ is the nonlinear function

$$G(x,\eta) = \begin{cases} 1 & x > \eta \\ 0 & -\eta \le x \le \eta \\ -1 & x < -\eta \end{cases}. \quad [5]$$

The parameter η is chosen as the value of V_{avg} when the NQR signal is absent. Based on a comparison of the magnitude of the the NQR measurements $V_{\text{avg}}(k)$ and $V_{\text{avg}}(k-1)$, the algorithm determines whether to increment or decrement the pulse width by the learning factor $\lambda(k)$.

The learning factor $\lambda(k)$ controls the rate at which the algorithm converges. When the pulse width is far from the optimal value it is desirable to use a large learning factor so that few iterations are needed to obtain a pulse width close to the optimal value. On the other hand, as the optimal value is approached, a smaller learning factor is desirable so that the search algorithm does not oscillate about the optimal value. For this reason, two different strategies were used for selecting the learning factor. The first approach uses a fixed learning factor $\lambda = 4$ μs. The second method uses an initial value of $\lambda(0) = 4$ μs, and then decrements this value by $\frac{1}{2}$ μs each iteration. The algorithm stops tuning the pulse width after the learning factor is decremented to zero.

Initial values for the pulse width $t_w(0)$ and gradient $\nabla_{t_w} J(0)$ must be specified at the start of the experiment. We chose an initial value for the pulse width that is smaller than the optimal value in order to conserve magnetization stored along the principal axis of the electric field gradient tensor. From Fig. 3, it is known that the steady-state optimal pulse width for a 1-ms pulse spacing is approximately 20 μs, and so we chose $t_w(0) =$

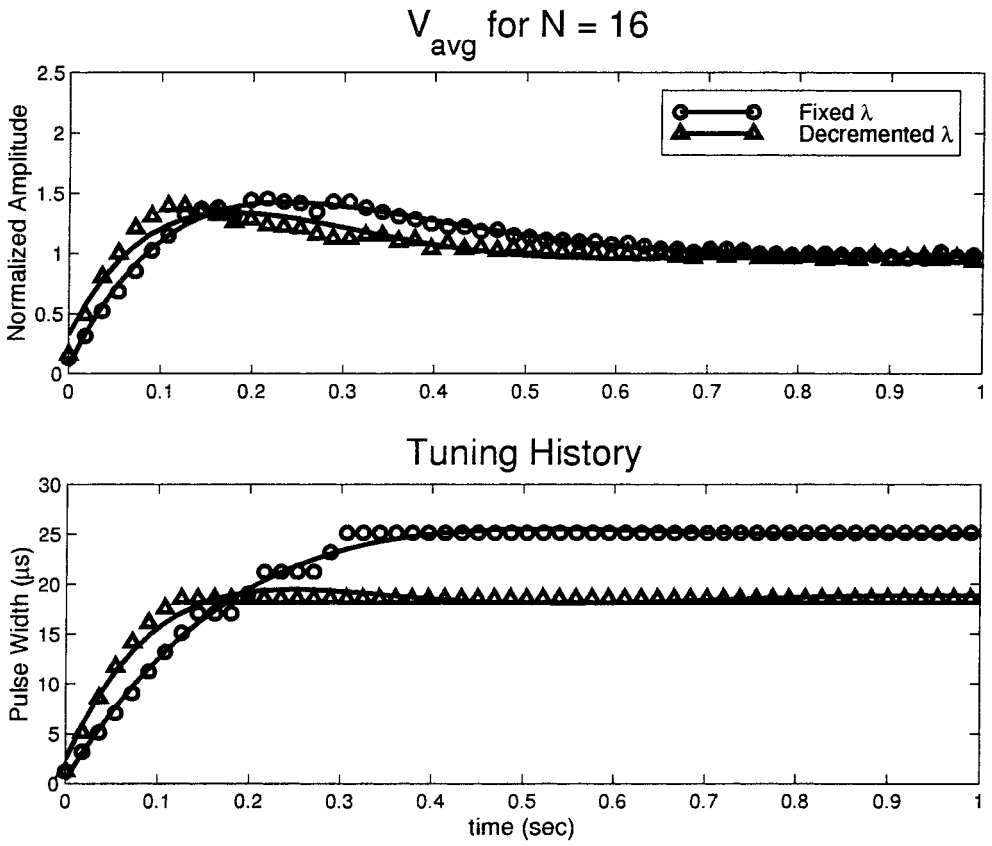

FIG. 5. Response of the SORC signal and tuning history for the case $N = 16$.

1 μs. The initial gradient is chosen as $\nabla_{t_w} J(0) = +1$ so that $t_w(1) > t_w(0)$.

Each learning method is evaluated for $N = 300$ and $N = 16$. In the case of $N = 300$, the interval between updates in pulse width is approximately equal to T_{1l}. When $N = 16$, the update time is approximately $3T_2$. Based on the transient response of the SORC sequence shown in Fig. 3, when $N = 300$ we expect the SORC signal to reach a steady-state between updates in pulse width, and as a result, do not anticipate that the peak value of V_{avg} will exceed the maximum steady-state value. In contrast, when $N = 16$, we expect a transient whose amplitude can exceed the maximum steady-state value.

3.3 Experimental Results

Figure 5 shows the normalized response V_{avg} and tuning history of t_w for each update strategy when $N = 16$. The vertical scale is normalized to the peak steady-state response obtained for the optimal pulse width of $t_w = 20$ μs. The algorithm that decrements the learning factor converges to within 1 μs of the optimal value. In contrast, the algorithm using a fixed learning factor produced a pulse width that is several microseconds greater than the optimal value. Note, however, that in both cases each algorithm produces a steady-state value near the maximum steady-state value. The fact that two different pulse widths can yield nearly the same steady-state response is evident from Fig. 3, which shows that the function describing the steady-state SORC response is flat near the optimal pulse width. Figure 5 reveals that the peak value of V_{avg} exceeded unity for both tuning algorithms. This result indicates that the SORC signal did not reach a steady-state waveform within the time interval of $N = 16$ pulses.

Figure 6 shows the normalized response V_{avg} and tuning history of t_w for each update strategy when $N = 300$. In this case both algorithms converge to a pulse width less than the optimal value and produce a steady-state value close to the maximum. In contrast to the results obtained for $N = 16$, the peak response does not exceed unity for either control algorithm. This observation is consistent with data shown in Fig. 4. Because the time interval for $N = 300$ pulses corresponds to T_{1l}, the SORC signal achieves a steady-state waveform between updates in pulse width.

4. DISCUSSION

We have demonstrated a feedback control algorithm that increases the SNR of an NQR measurement using the SORC sequence by automatically adjusting the pulse width. The algorithm is based on the gradient method, which determines the

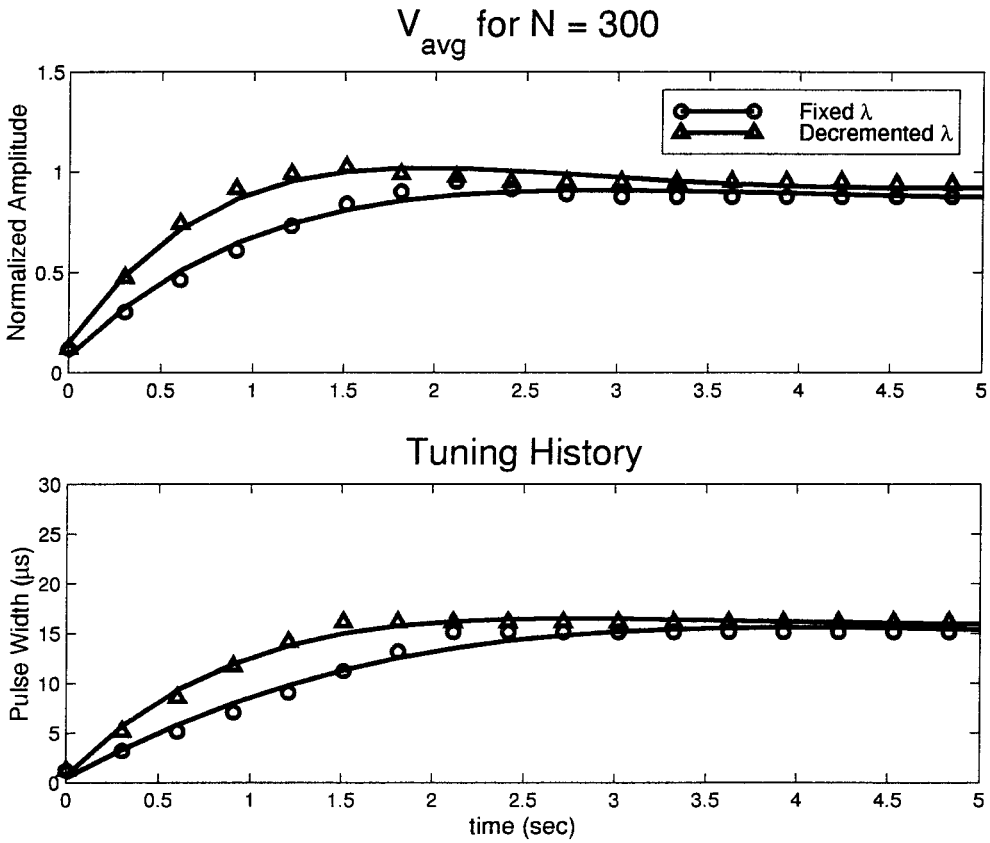

FIG. 6. Response of the SORC signal and tuning history for the case $N = 300$.

direction in which to adjust the pulse width in order to maximize the steady-state response. Despite its simplicity, the algorithm automatically adjusts the pulse width to a near optimal value within several iterations. The gradient method does not require either a parametric model of NQR dynamics or exact values of T_{l1}, T_2, and T_2^*. In addition, the algorithm uses a relative comparison between the magnitude of consecutive NQR measurements, thereby reducing the effects of noise.

The performance of the control algorithm can be improved by both decreasing the time required for the algorithm to estimate the optimal pulse width and minimizing the difference between the estimated and optimal pulse widths. Using other design tools, such as optimal or robust control techniques, it may be possible to achieve these goals. However, these approaches will require a model that describes the dynamic relationship between the pulse width $t_w(k)$ and response $V(k)$. Using standard identification techniques such as recursive least squares, we are currently developing a dynamic model that describes the response of the SORC signal to changes in pulse width.

The algorithm presented in this paper only adjusts the pulse width $t_w(k)$. It is also possible to optimize other parameters such as the pulse spacing or the frequency offset from resonance. The task of optimizing the pulse spacing is complicated by the fact that the steady-state relationship between SORC amplitude and pulse spacing is multipeaked (*7*). An algorithm for automatically optimizing the offset frequency is currently being studied.

In addition to automatically calibrating pulse parameters in an NQR detection system, feedback optimization may provide other advantages. Grechishkin developed a method for detecting the burial depth of land mines. In order to determine the burial depth, the frequency offset which maximizes the amplitude of the SORC signal must be determined (*2*). Feedback may provide a means for automatically determining the optimal offset frequency and hence an estimate of the mine depth.

5. CONCLUSION

Feedback control provides a means for automatically adjusting a pulse parameter to achieve a desired goal. It was demonstrated that measurements of the averaged NQR signal can be used to automatically adjust the pulse width in the SORC sequence so that the SNR of the NQR measurement is increased. The feedback algorithm, based on the gradient method, does not require knowledge of relaxation times or the amplitude of the RF pulse at the sample location. The use of feedback to automatically adjust a pulse parameter may be beneficial in applications beyond the one considered in this paper.

ACKNOWLEDGMENTS

This work is funded in part by the United States Army Construction Engineering Research Laboratories under Contract DACA 88-95-K-0002. The authors thank Dr. Robert Marino for his advice and suggestions during the course of this research.

REFERENCES

1. S. N. Subbarao, E. G. Sauer, and P. J. Bray, Nuclear quadrupole resonance in c-nitro compounds, *Phys. Lett.* **42A**(7), 461–462, (1973).
2. V. S. Grechishkin and S. N. Ya, New technologies: Nuclear quadrupole resonance as an explosive and narcotic detection technique, *Phys. Uspekhi* **40**(4), 393–406, (1997).
3. M. L. Buess, A. N. Garroway, and J. B. Miller, NQR detection using a meanderline surface coil, *J. Magn. Reson.* **92,** 348–362, (1991).
4. R. A. Marino and S. M. Klainer, Multiple spin echoes in pure quadrupole resonance, *J. Chem. Phys.* **67**(7), 3388–3389, (1978).
5. D. Ya. Osokin, Coherent multipulse sequences in nitrogen-14 NQR, *J. Mol. Struct.* **83,** 243–252, 1982.
6. W. S. Hinshaw, Image formation by nuclear magnetic resonance: The sensitive-point method, *J. Appl. Phys.* **47**(8), 3709–3721, (1976).
7. S. S. Kim, J. R. P. Jayakody, and R. A. Marino, Experimental investigations of the strong off-resonant comb (SORC) pulse sequence in ^{14}N NQR, *Zeitschrift Naturforschung A J. Phys. Sci.* **47A,** 415–420, (1992).
8. A. D. Hibbs, G. A. Barrall, P. V. Czipott, D. K. Lathrop, Y. K. Lee, E. E. Magnuson, R. Matthews, and S. A. Vierkotter, Landmine detection by nuclear quadrupole resonance, *in* (A. C. Dubey, J. F. Harvey, and T. Broach, Eds.), "Detection and Remediation Technologies for Mines and Minelike Targets III," Vol. 3392, pp. 522–532 (1998).
9. J. A. S. Smith and J. D. Shaw, Method of and apparatus for NQR testing selected nuclei with reduced dependence on a given environmental parameter. U.S. Patent Number 5583437, December 1996.
10. J. L. Schiano, A. G. Webb, and R. L. Magin, Flip angle optimization in fast MRI using adaptive feedback control, abstracts of the Society of Magnetic Resonance in Medicine, 10th Annual Meeting, San Francisco, CA, p. 1248 (1991).
11. P. S. Christy, R. C. Grimm, J. F. Greenleaf, and R. L. Ehman, Recursive RF excitation, *Magn. Reson. Med.* **26,** 361–367 (1992).
12. J. L. Schiano, A. G. Webb, and R. L. Magin, On-line optimization of an inversion-recovery pulse sequence using adaptive feedback control, 34th Experimental NMR Conference, St. Louis, MO, p. 28 (1993).
13. R. A. Marino, S. M. Klainer, and T. B. Hirschfeld, Fourier transform nuclear quadrupole resonance spectroscopy, *in* "Fourier, Hadamard, and Hilbert Transforms in Chemistry," pp. 147–182, Plenum Press, New York (1982).
14. E. Rodrigues and M. M. Rodrigues, Piezoelectric effects in nuclear-quadrupole resonance, *J. Chem. Phys.* **44,** 2200–2201, (1965).
15. R. S. Cantor and J. S. Waugh, Pulsed spin locking in pure nuclear quadrupole resonance, *J. Chem. Phys.* **73**(3), 1054–1063, (1980).
16. G. E. Karnaukh, B. B. Provotorov, and A. K. Khitrin, Thermodynamic theory of multipulse NQR experiments, *Soviet Phys. J. Exp. Theoret. Phys.* **57**(1), 93–96, (1983).
17. D. Ya. Osokin, V. L. Ermakov, R. H. Kurbanov, and V. A. Shagalov, The quasistationary states in multipulse NQR, *Zeitschrift Naturforschung A J. Phys. Sci.* **47A,** 439–445, (1992).
18. D. G. Luenberger, "Linear and Nonlinear Programming," 2nd ed., Addison–Wesley, Reading, MA (1984).
19. K. J. Astrom and Bjorn Wittenmark, "Adaptive Control," 2nd ed., Addison–Wesley, Reading, MA (1995).